

**The role of alkoxysilanes functional groups for surface modification of TiO₂ nanoparticles on non-isothermal crystallization of isotactic polypropylene composites****El papel de los grupos funcionales alcoxisilanos para la modificación de la superficie de nanopartículas de TiO₂ en la cristalización no isotérmica de compositos de polipropileno isotáctico**J.A. González-Calderón^a, M.G. Peña-Juárez^b, R. Zarraga^c, D. Contreras-López^e, J. Vallejo-Montesinos^{c*}^aCátedras CONACYT-Instituto de Física, Universidad Autónoma de San Luis Potosí, Manuel Nava #6, Zona Universitaria, C.P. 78290, San Luis Potosí, S.L.P. México.^bDoctorado Institucional en Ingeniería y Ciencia de Materiales. Universidad Autónoma de San Luis Potosí, Sierra Leona No. 550 Col. Lomas 2da. Sección, 78210 San Luis Potosí, SLP, México.^cDepartamento de Química, Universidad de Guanajuato, Noria Alta s/n, Guanajuato, Gto., 36050, México.^eDepartamento de Ingeniería Química, Universidad de Guanajuato, Noria Alta s/n, Guanajuato, Gto., 36050, México.

Received: September 5, 2020; Accepted: December 7, 2020

Abstract

Functionalization of fillers provides advantages in non-isothermal crystallization of isotactic polypropylene (iPP); therefore, kinetic properties of the crystallization of iPP composites filled with alkoxysilane-functionalized titanium dioxide (TiO₂) were investigated to understand the role of functional groups. The surface modification of TiO₂ nanoparticle was carried out with three different alkoxysilanes: 3-aminopropyltrimethoxysilane (APTMS), 3-chloropropyltrimethoxysilane (CPTMS) and 3-glycidoxypropyltrimethoxysilane (GPTMS); after, composites were prepared 0.5% by weight in iPP. The results of the X-Ray Diffraction and Nuclear magnetic resonance analyses showed the characteristic signals of each chemical species that confirm the success of surface modification of the oxide with alkoxysilanes. The study by Differential scanning calorimetry at different cooling rates allowed to observe that the non-isothermal crystallization of iPP composites is adequately described by Jeziorny's and Mo's equations; and that the addition of fillers of TiO₂ superficially modified with the alkoxysilanes changed the crystallization process thanks to the functional groups and their interface interactions with the polymer matrix; for example, the presence of CPTMS and GPTMS caused recrystallization of iPP and therefore, increased the crystallization process rate. Finally, the activation energy of the crystallization process of the composites varied depending on the alkoxysilane used, since less energy was needed for some cases; this probably due to better dispersion and that the particles acted as nucleation centers; therefore, facilitating the arrangement of the chains.

Keywords: Isotactic polypropylene, alkoxysilanes, non-isothermal crystallization, fillers, titanium dioxide.

Resumen

La funcionalización de rellenos, proporciona ventajas en la cristalización no isotérmica de polipropileno isotáctico (iPP); por lo tanto, se investigaron las propiedades cinéticas de los compositos de iPP rellenos con dióxido de titanio funcionalizado con alcoxisilanos (TiO₂), con el fin de comprender el papel de los grupos funcionales. La modificación de la superficie de nanopartículas de TiO₂ se realizó con tres alcoxisilanos diferentes: 3-aminopropiltrimetoxisilano (APTMS), 3-cloropropiltrimetoxisilano (CPTMS) y 3-glicidoxipropiltrimetoxisilano (GPTMS); después los compositos se prepararon al 0.5% en peso en iPP. Los resultados de los análisis de difracción de rayos X y resonancia magnética nuclear mostraron las señales características de cada especie química, lo cual confirma el éxito de la modificación de la superficie del óxido con alcoxisilanos. El análisis por calorimetría diferencial de barrido a diferentes velocidades de enfriamiento permitió observar que la cristalización no isotérmica de estos compositos de iPP está descrita adecuadamente por las ecuaciones de Jeziorny y Mo; y que la inclusión de rellenos de TiO₂ superficialmente modificado con alcoxisilanos cambió el proceso de cristalización gracias a los grupos funcionales y sus interacciones de interfaz con la matriz polimérica; por ejemplo, la presencia de CPTMS y GPTMS provocó una recristalización de iPP y, por lo tanto, aumentó la velocidad del proceso de cristalización. Finalmente, la energía de activación de los compositos varió dependiendo del alcoxisilano utilizado, ya que en algunos casos se necesitó menos energía; esto probablemente debido a una mejor dispersión y a que las partículas actuaron como centros de nucleación; por lo tanto, facilitaron la disposición de las cadenas.

Palabras clave: Polipropileno isotáctico; alcoxisilanos; cristalización no isotérmica; rellenos; dióxido de titanio.

* Corresponding author. E-mail: javas210@ugto.mx

<https://doi.org/10.24275/rmiq/Poly1995>

ISSN:1665-2738, issn-e: 2395-8472

1 Introduction

Currently, synthetic polymers are in a complicated situation. The origin of this situation is that polymers have a vast amount of applications resulting from their excellent properties and durability. And this durability is the reason behind the damage they cause to the environment (Auta, Emenike, & Fauziah, 2017; Vallejo-montesinos *et al.*, 2017; J. Vallejo-Montesinos, Muñoz, & Gonzalez-Calderon, 2016; Wright, Thompson, & Galloway, 2013). It is because of this that it has been currently studied how these materials can be degraded in a controlled way or the opposite case, increasing their useful life using various types of additives (Chiellini, Corti, D'Antone, & Baciú, 2006; Dintcheva *et al.*, 2015; Maryudi., Hisyam, Yunus, & Bag, 2013; Meer, Kausar, & Iqbal, 2016; Reingruber & Buchberger, 2010). Fillers have not only shown to promote any of the previously described actions but also to improve their thermo-mechanical properties, as already demonstrated (José Amir Gonzalez-Calderon, Pérez-Pérez, Pérez Rodríguez, Fierro-González, & Vallejo-Montesinos, 2019; Jagur-Grodzinski, 2006; Thomas, Thomas, & Bandyopadhyay, 2009). Nowadays, the two polyolefins with greater commercial and environmental importance due to a large number of applications and, therefore, wastes produced are polyethylene (PE) and polypropylene (PP).

Polyethylene is a semicrystalline polymer with various isomeric grades. PE is the most widely used general-purpose polymer, prevalent in the packaging sector, and is easy to reprocess (Mendes, Cunha, & Bernardo, 2011). Polypropylene (PP) is a semicrystalline thermoplastic, belonging to the polyolefins group, which is used in several applications such as food packaging, textiles, laboratory equipment, automobile components, and transparent films. For the reasons cited above, PP is considered one of the thermoplastic products that will have significant development in the future (J. A. Gonzalez-Calderon, Vallejo-Montesinos, Mata-Padilla, Pérez, & Almendarez-Camarillo, 2015; J. X. Li & Cheung, 1999; J. Vallejo-Montesinos *et al.*, 2016). Besides, the PP has a high resistance to chemical attack because it is essentially composed of carbon and hydrogen atoms. In some cases, it has a small presence of oxygen and nitrogen atoms that are incorporated into its structure during polymerization. However, PP is easily affected in the presence of

liquid hydrocarbons or chlorinated solvents that can cause cracking or swelling, as occurs with hot nitric or sulfuric acid that causes degradation (J. Vallejo-Montesinos *et al.*, 2016).

Isotactic polypropylene (iPP) is the most common commercial form for polypropylene. The reason behind this is due to its better mechanical properties derived from its higher degree of crystallinity. The high degree of crystallinity of iPP is associated with its more stereo-regular structure since all its methyl groups are oriented on one side of the carbon backbone. Therefore, the development of strategies to increase isotacticity in iPP has risen (Chûjô, Kogure, & Väänänen, 1994).

The iPP can have different crystalline phases. The relative content of the different phases depend on several factors such as stereochemical structure, molecular weight, crystallization temperature, the pressure applied during the crystallization process, and the addition of additives (Dai *et al.*, 2013; J. A. Gonzalez-Calderon, Vallejo-Montesinos, Almendarez-Camarillo, Montiel, & Pérez, 2016; J. A. Gonzalez-Calderon *et al.*, 2015; González, Pérez, Almendarez, Villegas, & Vallejo-Montesinos, 2016; J. Vallejo-Montesinos *et al.*, 2016; Z. Zhang, Wang, Junping, & Mai, 2012). The main crystalline phases are known as α -, β -, γ - and smectic or mesomorphic form (Alariqi, Kumar, Rao, & Singh, 2009; Ding *et al.*, 2012; González *et al.*, 2016; M. -R Huang, Li, & Fang, 1995; Lotz, 1998). The α form is the primary polypropylene form obtained under normal processing conditions (Chin & Ai Tjong, 1997; Ju *et al.*, 2016; Tang, Wang, Liu, & Belfiore, 2004; J. Vallejo-Montesinos *et al.*, 2016); however, the β phase is perhaps the most exciting phase for some applications due to its particular hardness and impact resistance properties (Huo, Jiang, An, & Feng, 2004; J. X. Li & Cheung, 1997; M. Li, Li, Zhang, Dai, & Mai, 2014; Lv, Huang, Kong, & Li, 2013; Mani, Chellaswamy, Marathe, & Pillai, 2016; Tang *et al.*, 2004; J. Vallejo-Montesinos *et al.*, 2016; C. Wang, Zhang, Du, Zhang, & Mai, 2011; Z. Zhang, Tao, Yang, & Mai, 2008).

Recently significant advances in particle modification have been reported. These investigations have allowed improvement in the efficiency of selective nucleation systems. Even new results have been obtained with titanium oxide particles, which had not been modified to achieve yields higher than 90% selectivity (J. A. Gonzalez-Calderon *et al.*, 2016, 2015; González *et al.*, 2016). The reinforcement of synthetic polymers has been the subject of several

studies to improve its specific properties. In this way, iPP has been enhanced with various fillers, with titanium dioxide (TiO₂) being one of the best options because, when it is included in the polymeric matrix, better electrical, optical, and mechanical properties are obtained (Karger-Kocsis, 1995). Besides, TiO₂ has the added value of being the primary inorganic pigment used in the coloration of plastics. On the other hand, this oxide is insoluble in most acids, which makes processing difficult since it requires large amounts of energy to achieve optimal dispersion in polymer matrices, due to the formation of agglomerates due to the highly attractive forces among particles (Mendoza, Peña-Juárez, Perez, & Gonzalez-Calderon, 2020). Surface modification is the most common strategy to minimize this attraction and to improve colloidal stability (Delgado Alvarado, Peña Juárez, Perez Perez, Perez, & Gonzalez, 2019). In particular, silanization has provided a chemical environment to the TiO₂ particles (Delgado Alvarado *et al.*, 2019; Mendoza *et al.*, 2020) that allow a decrease in the activation energy of the crystallization in iPP. Silane coupling agents can form a strong bond between organic and inorganic materials to generate heterogeneous environments or a uniform composite structure. Their characteristic composition allows two classes of functionality. (1) The hydrolyzable group forms stable condensation products with siliceous surfaces and other oxides such as those of aluminum, zirconium, tin, titanium, and nickel. (2) The organofunctional group alters the wetting or adhesion characteristics and significantly affects the Van der Waals forces between organic and inorganic materials. Recently, the use of organosilanes in polymers has increased interest due to their intrinsic characteristics such as heat-resistant, low toxicity, and environmentally stable materials for commercial applications as adhesion promoters, coupling, and crosslinking agents (Huber, Kelch, & Berke, 2016). These types of coupling agents interconnect different kinds of materials by forming strong chemical bonds to both inorganic materials and organic surfaces (Huber *et al.*, 2016; Pantoja, Encinas, Abenojar, & Martínez, 2013; S. Wang, Ahmad, & Mark, 1994), and these agents are competent at modifying the interface between the polymer and fillers (Koch, 1983). Also, surfaces with organosilanes attached alter the surface energy by improving the physical adhesion of polymers and fillers (Huber *et al.*, 2016). Alkoxysilanes have been used to form interpenetrating polymer networks with wheat-protein based materials (X. Zhang, Do, & Bilyk, 2007), to modify epoxide primers (Alyamac,

Gu, Soucek, Qiu, & Buchheit, 2012), to improve wood-polymer combinations (Schneider & Brebner, 1985). However little is known about the kinetics of the polymerizations and hydrolysis of these kinds of compounds (Issa & Luyt, 2019) which are responsible of their vast range of applications.

Besides, it has been reported elsewhere that organic-inorganic hybrid fillers are prepared using various alkoxysilane compounds (Cho *et al.*, 2016). These hybrid fillers could be promising as nucleating agents since they enhance the crystallinity of iPP. Also, the mixture of polymer and alkoxysilanes can improve the adhesion at the organic-inorganic interface of the composites (Lee, Joo, & Gong, 2005). For the reasons cited above, the type of organosilane used as a coupling agent is crucial since it could impact the crystallization process. It is expected that the functional groups on the filler surfaces play a critical role in the final structure of the polymer composites since they profoundly influence the interface interactions of the filler with the polymer matrix (He *et al.*, 2020). Also, silane coupling agents such as alkoxysilanes have been proved in polymer matrices such as iPP, finding that they can enhance mechanical properties such as tensile strength (Demir, Balköse, & Ülkü, 2006; Fuad, Ismail, Ishak, & Omar, 1995; Ismail, Mega, & Abdul Khalil, 2001), thermal conductivity (Demir *et al.*, 2006; Muratov, Kuznetsov, Il'inykh, Burmistrov, & Mazov, 2015).

A vital part of the formation of the crystals by fillers is the modification itself. Previously, it was observed that the silanization provides a chemical environment to the TiO₂ particles that allow a decrease in the energy of activation of the crystallization in iPP (José Amir Gonzalez-Calderon *et al.*, 2019). These results, which are opposite to another corresponding to the use of fillers functionalized with dicarboxylic acids, have opened a new question: how does the lateral group of a chemical reagent affect the crystallization process in the iPP composites? Also, a full investigation of the influence of filler functional groups on the non-isothermal crystallization of iPP composites remains absent. Three representative silane coupling agents with different functional groups are of our particular interest: 3-aminopropyltrimethoxysilane (APTMS), 3-chloropropyltrimethoxysilane (CPTMS) and 3-glycidoxypropyltrimethoxysilane (GPTMS) (Koch, 1983; Sterman & Marsden, 1966). APTMS is widely used to improve the dispersion in aqueous systems (Delgado Alvarado *et al.*, 2019; J A Gonzalez-Calderon, Vallejo-Montesinos, Martínez-Martínez,

Cerecero-Enríquez, & López-Zamora, 2019; López-Zamora, Martínez-Martínez, & González-Calderón, 2018; Javier Vallejo-Montesinos, Gámez-Cordero, Zarraga, Pérez Pérez, & Gonzalez-Calderon, 2019). CPTMS has interesting uses in catalytic systems and for metal ions capture (Allen, Rosenberg, Johnston, & Hart, 2012; Habila *et al.*, 2020): Lastly, GPTMS has exciting features derived from its epoxide group that can be used with biological macromolecules (Connell *et al.*, 2017; Shirotsaki *et al.*, 2009; Tonda-Turo *et al.*, 2011). Therefore, in this work, these three alkoxysilanes were chosen due to their different nature caused by the side group. A bonus is that the modification with alkoxysilanes can be done in less toxic solvents than the ones used in dichlorosilanes. The importance of these three is to assess how does the functional group of a chemical reagent affects the crystallization process in iPP composites. All three had the same alkoxysilane structure and varied only in the terminal group of the propyl chain. In this work, the effect of 3 different alkoxysilanes on the non-isothermal crystallization of isotactic polypropylene was evaluated to demonstrate that the terminal of the functional groups has a direct impact on the behavior of this process. By assessing the kinetic parameters and the activation energy, it was shown that the crystallization rate could be modulated as well as the energy requirements to carry out this process.

2 Materials and methods

2.1 Materials

Isotactic polypropylene (MFI = 35 g/10 min at 230 °C and 2.16 kg, ASTM D 1238) was supplied by Sigma Aldrich, 3-aminopropyltrimethoxysilane (APTMS) 97%, 3-chloropropyltrimethoxysilane (CPTMS) 97% and 3-Glycidoxypropyltrimethoxysilane (GPTMS) 97% were supplied by Sigma Aldrich. Commercial titanium dioxide particles (TiO₂) were supplied by DuPont (R-104). KEM supplied ethanol, methanol, and xylene.

2.2 Silanization of the TiO₂ surface by trimethoxysilanes

As reported elsewhere, the typical modification procedure was as follows, 2 g of TiO₂ particles were dispersed in 25 g of ethanol and stirred at room temperature for one h. Later the solution was

sonicated for 30 min. To the above mixture, 4 g of alkoxysilane (APTMS/GPTMS/CPTMS) was added in a 10 min interval, and then the mixture was refluxed for another six h. This solution was filtered and the precipitate washed several times with water and methanol to remove the unreacted alkoxysilane. The obtained particles were subsequently dried in an oven at 60 °C for 24 h to remove the residual solvent (J A Gonzalez-Calderon *et al.*, 2019; López-Zamora *et al.*, 2018), and identified as follows: TiO₂ functionalized with CPTMS labeled as TiO₂-Cl; TiO₂ with GPTMS as TiO₂-G; and TiO₂ with APTMS as TiO₂-NH₂.

2.3. Preparation of iPP composites by solution and non-isothermal crystallization

iPP/TiO₂-Cl, iPP/TiO₂-NH₂, and iPP/TiO₂-G composites of 0.5% of mass were prepared by solution of 10 g of iPP/TiO₂ with 100 mL of xylene at 120 °C and 400 rpm. The corresponding solution was dried at 100 °C for 24 h to remove any sign of the solvent. The composites were later dried one week in an oven at 60 °C to remove any traces of solvent. This led to fine powder that was later dried and kept away from light exposure. To perform a non-isothermal crystallization analysis, the study was conducted on a TA Instruments model Q2000 differential scanning calorimeter (DSC) in a dry nitrogen atmosphere. About 10 mg of the composites, were melted at 200 °C and maintain an isothermal step for 10 min as a means to delete the thermal and mechanical memory of the composite, finally cooling at different constant rates of 2.5, 5, 10 and 20 °C min⁻¹. The equipment recorded all the exothermal curves of heat flow as functions of temperature.

2.2.1 Non-isothermal crystallization kinetics

As in previous studies, the Avrami equation initially stated for the isothermal crystallization process was used:

$$X_t = 1 - e^{-Z_t t^n} \quad (1)$$

where X_t refers to the relative crystallinity, the term n relates to a mechanism constant, Z_t is a composite rate constant (here the information about nucleation and growth rate parameter is contained), and finally t is the crystallization time. The relative crystallinity X_t is derived from the following equation:

$$X_t = \frac{\int_{t_0}^t (dH_c/dt) dt}{\int_{t_0}^{t_\infty} (dH_c/dt) dt} \times 100 \quad (2)$$

In this approach, the enthalpy of the crystallization generated during an infinitesimal time range (dH_c) is integrated over a lapse time that ranges from an onset time t_0 to an end time of t_∞ , respectively. Eq. 1 is then expressed in their logarithmic form as:

$$\log(-\ln(1 - X_t)) = \log Z_t + n \log t \quad (3)$$

The previous equation allows estimating Z_t ; however, for this model to be suitable for a non-isothermal process, Z_t must be adequately corrected to consider cooling rate, φ , of the polymer. For this case, the Jeziorny correction is used and assumes a constant or almost constant φ ; therefore, the equation for the non-isothermal crystallization kinetics remains as:

$$\ln Z_c = \frac{\ln Z_t}{\varphi} \quad (4)$$

As stated, before for this model is sustained in the assumption that a non-isothermal process is an integration over an infinite number of small isothermal steps:

$$1 - X_T = e^{-\frac{K(T)}{\varphi^m}} \quad (5)$$

where $K(T)$ is the cooling function, m corresponds to an Ozawa exponent (which is related to the dimension of the crystal growth). To further adequate to all kind of systems, it is common to combine Eqs 1 and 5 to produce the following:

$$\ln(\varphi) = \ln F(T) - a \ln t \quad (6)$$

and

$$F(T) = [K(T)/Z_t]^{1/m} \quad (7)$$

where the logarithm of the cooling rate was obtained as the difference between $F(T)$ (which is defined as the value of cooling rate that is the cause of a defined crystallinity degree over a unit crystallization time) and the product of the ratio of the Avrami exponent a and the logarithm of the crystallization time t . $F(T)$ is the ratio between the cooling function $K(T)$ and the Jeziorny term (Z_t) elevated to the inverse of the Ozawa exponent (m).

The Kissinger method was used to estimate the change in the activation energy (ΔE) of the crystallization process using an iso-conversional method, as proposed by Friedman and Vyazovkin (Blaine & Kissinger, 2012a; Kissinger, 1956). This method associates the variation of the crystallization peak temperature with the cooling rate obtained by a correlation value of ΔE , according to the

following (Blaine & Kissinger, 2012b; Dai *et al.*, 2015; L. Huang, Wang, Wang, Wang, & Song, 2016; Kissinger, 1956; Papageorgiou & Panayiotou, 2011; Vyazovkin, 2002):

$$\ln \left(\frac{dX}{dt} \right)_{X,i} = A - \frac{\Delta E_X}{RT_{X,i}} \quad (8)$$

being ΔE_X the neat activation energy at a specific conversion, X , using an instantaneous crystallization rate $(dX/dt)_{X,i}$ at a spectrum of temperatures for that conversion $T_{X,i}$ changing the cooling rates (i).

2.3 ^{13}C , ^{29}Si NMR (Nuclear Magnetic Resonance) characterization

^{13}C , ^{29}Si , NMR spectra of the TiO_2 functionalized particles were obtained using a Bruker Ascend (400 MHz) equipment (^{29}Si) in solid-state. For ^{13}C NMR, the parameters were the following: 20480 scans with an acquisition time of 0.0339 with a cp pulse sequence with a relaxation delay of 4s. For ^{29}Si NMR, the parameters were the following: 12288 scans with an acquisition time of 0.0639 with a cp pulse sequence with a relaxation delay of 4s and a pulse width of 4 μs .

2.4 XRD Characterization of the modified TiO_2 particles

To further confirm the crystalline structure of the functionalized systems was kept, an X-ray diffraction spectroscopy (XRD) analysis was performed. The samples were prepared using a mortar to grind up finely the TiO_2 powders. The particles were characterized using an Equinox System Equip (Inel 081D Model with XRG 3000D Program) in a 2θ range of 5 to 80°.

3 Results and discussion

3.1 XRD characterization of the samples

In Figure 1, XRD patterns exhibited sharp diffraction peaks at 25° (101), 38° (004), and 49° (200), which refers to the TiO_2 crystalline structure (Thamaphat, Limsuwan, & Ngotawornchai, 2008). It is well-noted that the modification did not affect the crystallinity of the TiO_2 particles since the typical pattern for TiO_2 was maintained for all three functionalizations, $\text{TiO}_2\text{-Cl}$, $\text{TiO}_2\text{-NH}_2$, and $\text{TiO}_2\text{-G}$, as reported everywhere.

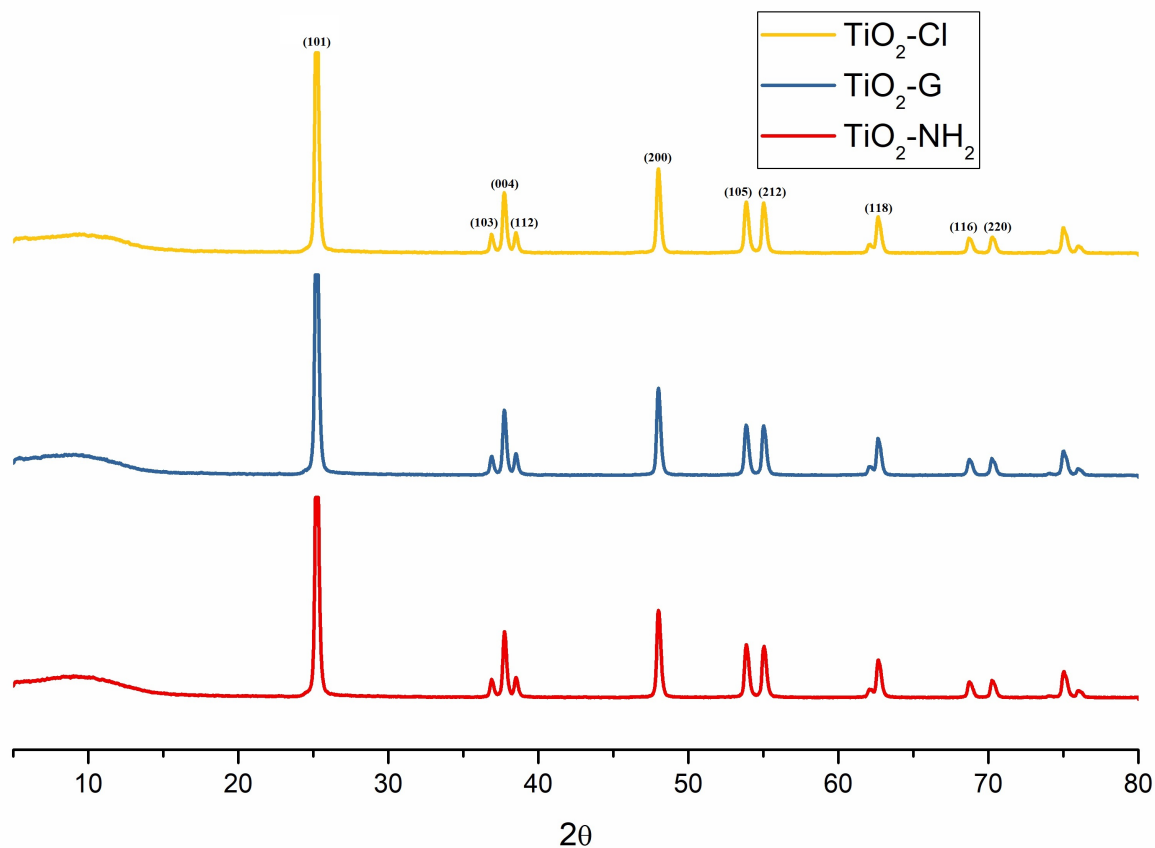


Fig. 1. XRD Pattern for the TiO_2 particles. $\text{TiO}_2\text{-C}$ stands for $\text{TiO}_2\text{-Chloride}$, $\text{TiO}_2\text{-G}$ holds for $\text{TiO}_2\text{-Glycidoxo}$, and $\text{TiO}_2\text{-NH}_2$ stands for $\text{TiO}_2\text{-Amine}$.

The conservation of the DRX pattern implies that the functionalization was performed only on the surface of the metal oxide that the siloxane coating is skinny in-depth (Ijadpanah-saravi, Safari, & Khodadadi-darban, 2014; Tong, Zhang, Tian, Chen, & He, 2008)

3.2 NMR Characterization of the siloxane coating

In Figures 2 and 3, the ^{13}C and ^{29}Si NMR spectra of the functionalized particles are presented. As it is visible in figure 2, $\text{TiO}_2\text{-NH}_2$ exhibited the following chemical shifts: 10, 22, and 41 ppm that correspond to the presence of the 3-aminopropyl groups: (1) $\text{-Si-CH}_2\text{-}$, (2) $\text{-CH}_2\text{-}$ and (3) $\text{-CH}_2\text{-NH}_2$, respectively; while $\text{TiO}_2\text{-Cl}$ showed signals at 10, 26 and 47 ppm for the 3-chloropropyl groups attached to the atom: (1) $\text{-Si-CH}_2\text{-}$, (2) $\text{-CH}_2\text{-}$ and (3) $\text{-CH}_2\text{-Cl}$ (Allen *et al.*, 2012;

Cao, Zuo, Wang, Zhang, & Feng, 2017; Habila *et al.*, 2020); and finally, for $\text{TiO}_2\text{-G}$ in there were peaks at 9, 23, 42, 50 and 71 ppm, which are associated with the glycidoxo group: (1) $\text{-Si-CH}_2\text{-}$, (2) $\text{-CH}_2\text{-}$, (5) $\text{-O-CH}_2\text{-}$, (4) -O-CH- and (3) $\text{-CH}_3\text{-O}$ (Kesmez, 2020; Nocuń, Siwulski, Leja, & Jedliński, 2005; Shirosaki *et al.*, 2009; Tonda-Turo *et al.*, 2011). Besides there was a shift at 127 ppm that can be attributed to solvent traces (xylene). For the ^{29}Si NMR spectrum of the functionalized particles (see Figure 3), $\text{TiO}_2\text{-NH}_2$ showed two chemical shifts at -54 and -68 ppm, $\text{TiO}_2\text{-Cl}$ had chemical shifts at -58 and -68 ppm, finally $\text{TiO}_2\text{-G}$ showed the same shifts at -59, and -67 ppm. These shifts are a clear indication of the T units (T2 and T3) present in the particles (Cao *et al.*, 2017; Tonda-Turo *et al.*, 2011; Uhlig & Dortmund, 2000; Javier Vallejo-Montesinos *et al.*, 2019). With the results obtained from the spectra of the TiO_2 particles, the success of the functionalization with alkoxy silanes was confirmed.

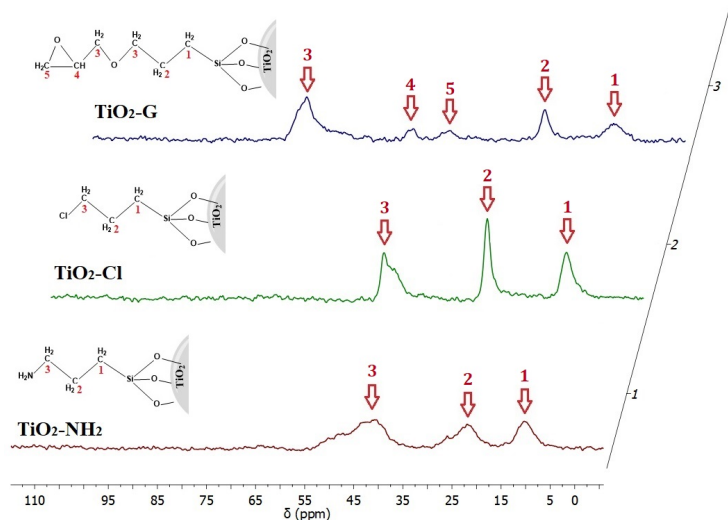


Fig. 2. ^{13}C NMR spectra of the functionalized TiO_2 particles. 1) stands for $\text{TiO}_2\text{-NH}_2$, 2) holds for $\text{TiO}_2\text{-Cl}$, and 3) $\text{TiO}_2\text{-G}$.

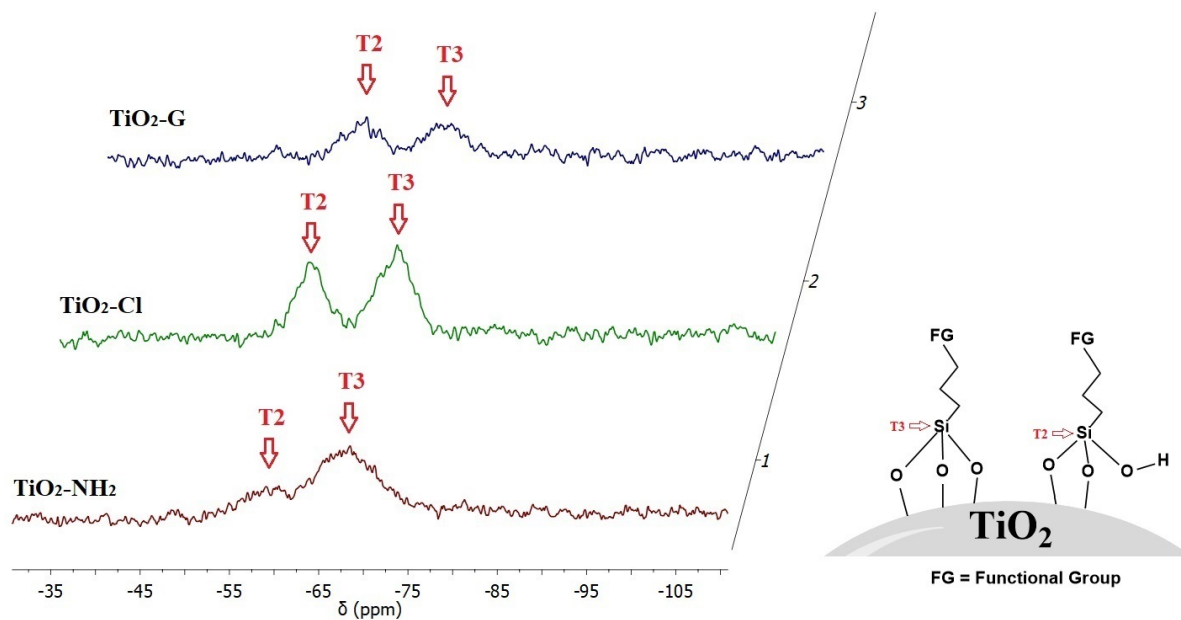


Fig. 3. ^{29}Si NMR spectra of the functionalized TiO_2 particles. 1) stands for $\text{TiO}_2\text{-NH}_2$, 2) holds for $\text{TiO}_2\text{-Cl}$, and 3) $\text{TiO}_2\text{-G}$.

3.3 Analysis: Non-isothermal crystallization of iPP

The behavior of iPP and the modified composites, iPP/ TiO_2 , iPP/ $\text{TiO}_2\text{-Cl}$, iPP/ $\text{TiO}_2\text{-NH}_2$, and iPP/ $\text{TiO}_2\text{-G}$ under a non-isothermal crystallization process was investigated under different cooling rates (2.5, 5, 10, and 20 $^\circ\text{C}/\text{min}$). As is well-known, the crystallization of polymers consists of two stages: first in the nucleation step, the centers of the new

phase are formed, and secondly, they will begin to grow, and new layers of crystals will be deposited on the primary nuclei, thus expanding the dimensions of the crystalline phase. In this work the crystallization process are reported in Figure 4 by means of thermograms as function of cooling rates (ϕ). As can be seen, the crystallization curves shifted to lower temperatures and became narrower as the cooling rate increased. This behavior is due to the fact that in slow cooling, the crystallization temperature is higher,

therefore, the growth rate is upper and more dominant than the nucleation rate; which means that few nuclei will form and grow very fast. (Ding *et al.*, 2012; Supaphol, Thanomkiat, Junkasem, & Dangtungee, 2007). While, when the cooling temperature is low, the nucleation rate is more dominant, and many nuclei are forming and growing at a slower rate (Gonzalez-Rodriguez, Escobar-Barrios, Peña-Juárez, & Pérez, 2020). Furthermore, once the fillers were included, the crystallization curves showed different behaviors depending on the type of filler into the iPP matrix, however all of them shifted to higher temperatures. It is well-noted that the influence of pristine TiO₂ and TiO₂-NH₂ (Figure 4b and 4c) on the polymer crystallization is low in comparison with the other two fillers; all curves and T_c for all for cooling rates are similar to pure iPP. Nevertheless, it was possible to see that during the non-isothermal crystallization, the temperature for these composite shifted towards higher temperature; with this behaviour, it is possible to state that this filler is acting as heterogeneous nuclei, which could which could reduce the crystallization time of the iPP (Raka & Bogoeva-Gaceva, 2017; J. Wang & Dou, 2007).

On the other hand, TiO₂-Cl, and TiO₂-G systems presented a shoulder at lower temperature for all heating rates. This phenomenon is commonly called

secondary crystallization because the intercrystalline amorphous polymer crystallizes at the end of the process, creating an added broadening or shoulder on the DSC exotherm (Borovanska, Dobрева, Benavente, Djoumalisky, & Kotzev, 2012). In particular, for these two types of fillers (Chloride and Glicidoxy, respectively), the presence of this shoulder may be due to the specificity of polypropylene crystal melting, also called as melting recrystallization of the forming crystals, to the presence of a different phase, or to the presence of fillers that are resulting in the retardation of chain mobility.

Figure 5 shows the relative crystallinity of iPP and its composites, iPP/TiO₂, iPP/TiO₂-Cl, iPP/TiO₂-NH₂, and iPP/TiO₂-G at different crystallization cooling rates as a function of time. It is possible to observe sigmoid curves in all graphs, which shift to the left when the rate increased since the time for crystallization was reduced. The reason of this is that when the polymer matrix is cooled at low speed, the crystalline part of the polypropylene can be ordered forming nucleation centres, increasing the rate at which the formation of the crystals occurs; while at high speeds, the process occurs very fast (J.A. Gonzalez-Calderon, Vallejo-Montesinos, Almendarez-Camarillo, Montiel, & Pérez, 2016).

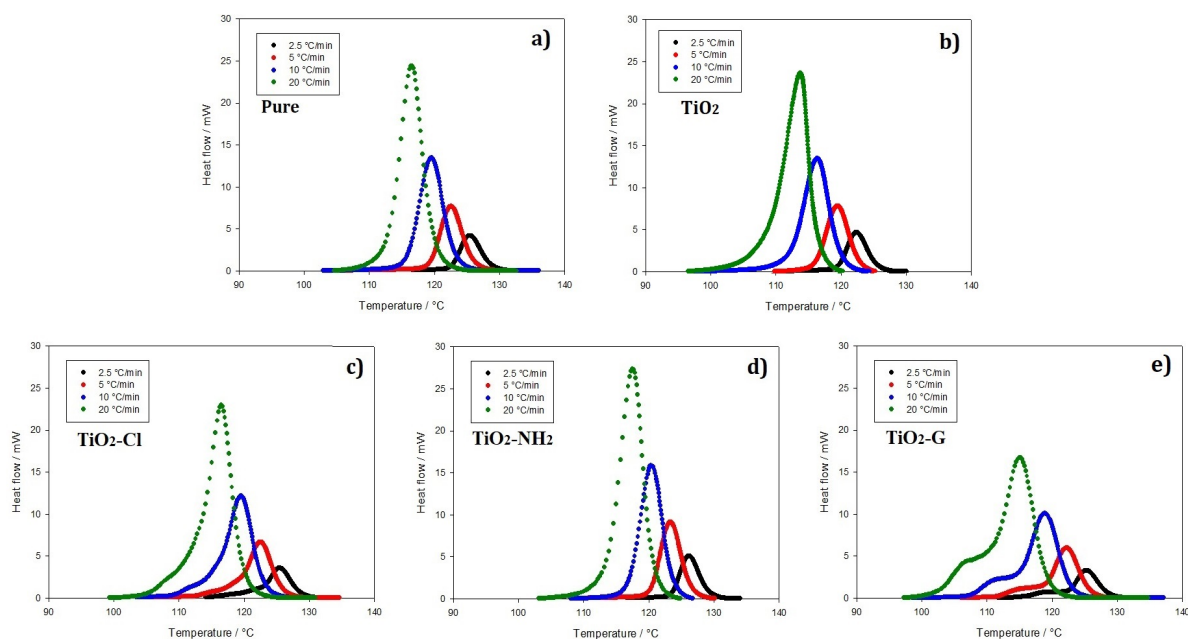


Fig. 4. Non-isothermal crystallization thermograms for iPP composites under different crystallization cooling rates for a) pure iPP, b) iPP/TiO₂, c) iPP/TiO₂-Cl, d) iPP/TiO₂-NH₂ and e) iPP/TiO₂-G.

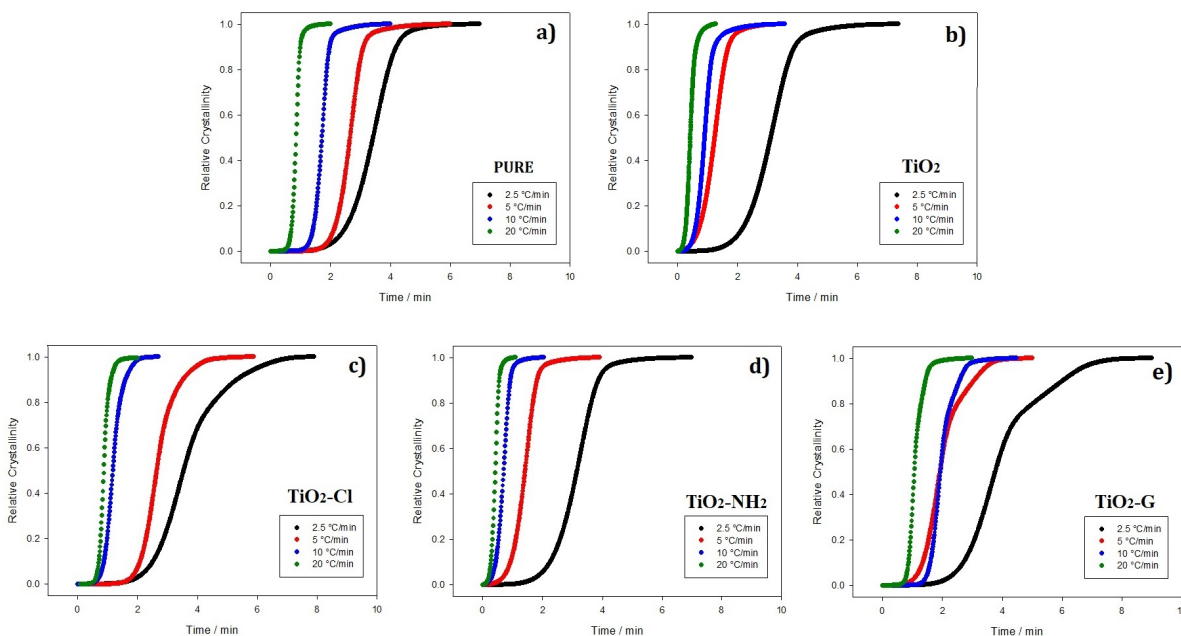


Fig. 5. Relative crystallinity of iPP composites as a function of crystallization time under different crystallization cooling rates for a) pure iPP, b) iPP/TiO₂, c) iPP/TiO₂-Cl, d) iPP/TiO₂-NH₂ and e) iPP/TiO₂-G.

Regarding the influence of fillers, it was seen that the TiO₂ and TiO₂-NH₂ systems presented a curious behaviour, while at low cooling rate the crystallization time remained almost the same as pure iPP, at high rate it decreased significantly. With this, it is possible to infer that this type of filler acts as heterogenous nuclei only at faster cooling, since the nucleation rate dominates the crystallization process and reduces the time for crystallization. While, as previously observed, the addition of fillers based on TiO₂-Cl and TiO₂-G greatly affected the non-isothermal crystallization process. As observed for these systems, the composite polymers increased the time of the crystallization process, this due to a secondary crystallization was carried out.

The total crystallinity of the composites at each cooling rate was calculated with the help of a Universal Analysis software. The crystallinity degree X_c was estimated using the following equation:

$$X_c(\%) = \frac{\Delta H_m}{\Delta H_m^* \cdot \omega} \quad (9)$$

ΔH_m is melting enthalpy of each composite evaluated by DSC, ΔH_m^* is the melting enthalpy for 100% crystalline iPP, equals to 209 J g⁻¹; and ω is the weigh fraction of iPP in the sample.

The calculated crystallinity (X_c) for the thirteen samples are reported Table 1. According to the results, X_c for pure iPP is around 51.1 - 58.0%, and interestingly, it could be seen that this increased with higher cooling rate. This behavior was observed also for the composites: iPP/TiO₂, iPP/TiO₂-Cl and iPP/TiO₂-NH₂. In addition, it was possible to observe a clear effect of the fillers; when TiO₂-Cl and TiO₂-NH₂ were used, the crystallinity increased to 59.7 - 60.7% and 52.7 - 59.9%, respectively. This phenomenon can be explained as these fillers act better as effective nucleation centers and so, the crystals can growth around them. On the other hand, the composites with TiO₂ and TiO₂-G practically decreased the amount of crystals, when compared to pure iPP. With this, it is possible to state that the functional group of each alkoxy silane has a great effect in the crystallization of iPP; first because pristine TiO₂ is not an effective nucleation filler by itself; while TiO₂-G hinders the arrangement of the chains, decreasing the crystal content. Nevertheless, the TiO₂-Cl and TiO₂-NH₂ systems do promote the incorporation of the chains, improving the efficiency of the crystallization process, thanks to their distinctive chemical properties.

Table 1. Total crystallinity of studied samples by DSC for iPP and its composites.

	Cooling rate °C min ⁻¹	Total crystallinity X_c %
Pure iPP	2.5	51.1
	5	53.2
	10	56.7
	20	58
iPP/TiO ₂	2.5	52.3
	5	54.7
	10	54.1
	20	54.4
iPP/TiO ₂ -Cl	2.5	59.4
	5	61.8
	10	60.6
	20	60.4
iPP/TiO ₂ -NH ₂	2.5	52.4
	5	59.2
	10	63
	20	59.6
iPP/TiO ₂ -G	2.5	55.4
	5	51.5
	10	52.8
	20	53.7

3.3.1 Non-isothermal crystallization kinetics

The kinetics parameters of the non-isothermal crystallization process were obtained according to Jeziorny's (Eq. 4) and Mo's (Eq. 5) methods. The results were plotted and included for neat iPP and its composites in Figure 6, and the corresponding data of these crystallization parameters are summarized in Table 2. It is well noted that straight lines were obtained for most cooling rates, which means that this method is suitable to describe this non-isothermal crystallization process. Also, it is observed that high cooling rates (ϕ) accelerate the process, reducing the crystallization time, this because many nucleation centers are forming very fast. First, for pure iPP, iPP/TiO₂ and iPP/TiO₂-NH₂ systems, only one straight line was obtained, which means that the crystallization for these systems can be effectively described by Jeziorny's method and corresponds to a single stage of crystallization. According to the Avrami coefficient, n , just with the inclusion of pristine TiO₂, the iPP crystallization became a easier process, since the value decreased and was closed to 3, indicating a three-dimensional crystal growth.

On the other hand, the effect of the TiO₂-Cl and TiO₂-G fillers is observed by an inflection point found in each line. This inflection point corresponds to a two-stage crystallization process.

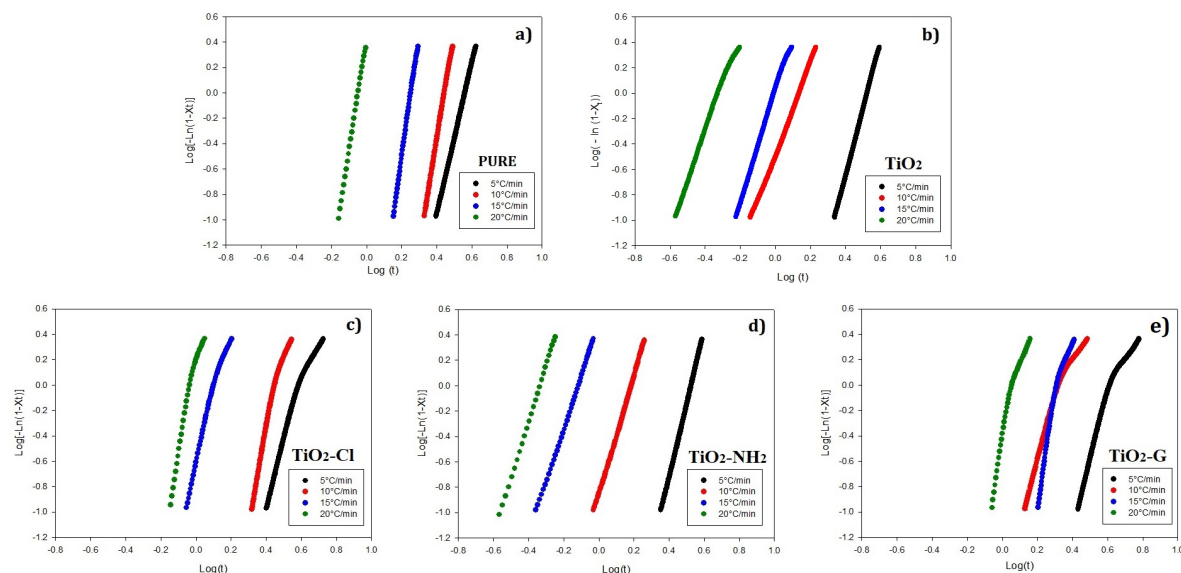
Fig. 6. Plots of $\log(-\ln(1 - X_t))$ versus $\log(t)$ for iPP composites under different crystallization cooling rates for a) pure iPP, b) iPP/TiO₂-Cl, c) iPP/TiO₂-NH₂ and d) iPP/TiO₂-G.

Table 2. Non-isothermal kinetic parameters from the Jeziorny model for iPP and its composites.

	Cooling rate/ °C min ⁻¹	<i>n</i>	<i>Z_t</i>	<i>Z_c</i>
Pure iPP	2.5	5.96	0.0005	0.05
	5	8.34	0.0002	0.18
	10	9.65	0.004	0.57
	20	8.91	2.679	1.05
iPP/TiO ₂	2.5	5.33	0.002	0.08
	5	3.66	0.326	0.8
	10	4.38	1.054	1.01
	20	3.78	1.153	1.15
iPP/TiO ₂ -Cl	2.5	5.32	0.001	0.06
	2.5	2.35	0.045	0.29
	5	7.59	0	0.21
	5	3.28	0.038	0.52
	10	6.31	0.241	0.87
	10	3.21	0.519	0.94
	20	8.68	2.09	1.04
	20	3.61	1.571	1.02
iPP/TiO ₂ -NH ₂	2.5	5.8	0.001	0.06
	5	4.7	0.136	0.67
	10	4.17	3.078	1.12
	20	4.5	32.21	1.19
iPP/TiO ₂ -G	2.5	5.59	0	0.04
	2.5	1.82	0.086	0.37
	5	5.07	0.025	0.48
	5	1.82	0.301	0.79
	10	9.56	0.001	0.51
	10	3.04	0.129	0.81
	20	8.79	0.386	0.95
	20	3.24	0.699	0.98

As can be seen in Table 2, in the first stage of crystallization, the *n* varies from 5.32 to 8.68 for iPP/ TiO₂-Cl and from 5.59 to 8.79 for iPP/ TiO₂-G, indicating a complex crystallization process for the first stage of crystallization. In contrast, the second crystallization stage is a more straightforward process since the *n* exponent had lower values from 2.35 to 3.61 for chlorine and from 1.82 to 3.24 for Glicidoxo (Kaya, McNally, Douglas, Coburn, & Gupta, 2018). Finally, it is observed that the *Z* values for all systems increase as the cooling rates rise; this confirms that the crystallization process was carrying out faster for 15 and 20 °C/min. The more outstanding Avrami exponent was found for the iPP/ TiO₂-NH₂, indicating that this was the fastest process of all composites and that this filler acted as nucleation centers (Gonzalez-Rodriguez *et al.*, 2020).

F(T) was obtained according to Eq. 6 (Mo model), and the values ranging from 10% to 90% in 20% intervals are summarized in Table 3. In this table, it is possible to observe that when the crystallinity increased (*X_t*), the value of *F(T)* was higher because a higher degree of crystallinity requires an upper heating rate to achieve a defined crystallinity in a unit of crystallization time due to it is more difficult to form the subsequent crystal when the amount of already started crystals is higher.

With this information, it is possible to state that pristine TiO₂ did not act as an effective nucleation center, since very similar values were obtained when compared to pure iPP. On the other hand, there is a different effect depending on the type of filler; for example, smaller values for *F(T)* is needed for the iPP/ TiO₂-G composites than for pure iPP, probably due to the melting recrystallization of the forming crystals (Borovanska *et al.*, 2012). While for the iPP/ TiO₂-Cl and the iPP/ TiO₂-NH₂ composites, only a little increase was observed. Therefore, the differences observed for *F(T)* indicate that the mechanism of growth of crystals and the crystallization process depends on the type of filler (J. A. Gonzalez-Calderon *et al.*, 2016).

3.3.2 Effective activation energy from the non-isothermal analysis

The effective activation energy (ΔE_X) calculated through the iso-conversional Friedman treatment from Eq. 8 for iPP and its composites was plotted and presented in Figure 7, in which it is possible to observe that the crystallization rate increased when the temperature decreased, according to the obtained negative values.

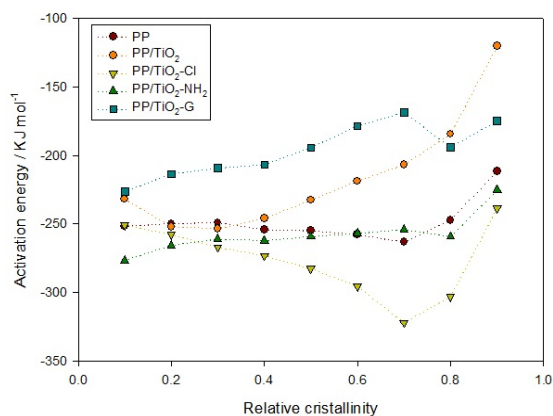


Fig. 7. Activation energy behavior as a function of crystallinity degree for iPP and its composites.

Table 3. Non-isothermal kinetic parameters from the Mo model for iPP and its composites.

	$X_t/\%$				
	10	30	50	70	90
<i>Pure iPP</i>					
$F(t)$	4.998	6.19	6.952	7.721	8.671
a	0.61	0.64	0.66	0.68	0.69
<i>iPP/TiO₂</i>					
$F(t)$	4.973	6.686	7.862	9.025	11.382
a	1	1.05	1.07	1.09	1.16
<i>iPP/TiO₂-Cl</i>					
$F(t)$	5.038	6.303	7.228	8.406	11.235
a	0.67	0.7	0.72	0.75	0.79
<i>iPP/TiO₂-NH₂</i>					
$F(t)$	5.114	6.424	7.128	7.737	8.619
a	1.01	0.99	0.97	0.95	0.94
<i>iPP/TiO₂-G</i>					
$F(t)$	3.717	4.889	5.697	6.699	10.095
a	0.46	0.52	0.54	0.57	0.64

Besides, the influence of the fillers within the iPP matrix is appreciated in the crystallization process since for the iPP/TiO₂-Cl and iPP/TiO₂-NH₂ systems less energy was needed than for pure iPP; because they disperse better and can act as effective nucleation centers, and therefore, they order and arrange the chains correctly. Different behavior was observed for the iPP/TiO₂ and iPP/TiO₂-G systems, these two composites needed more energy during the crystallization. According to the above, pristine TiO₂ does not work as an effective nucleation center by itself, and on the contrary, it hinders the arrangement of the chains. Finally regarding iPP/TiO₂-G, in addition to its poor nucleation ability, its behavior can be attributed to the secondary crystallization found in Figure 4d). In the melting recrystallization of the forming crystals, migration of molten chains over the crystallized mass became more difficult due to the glycidoxy group. Instead of favoring crystallization, it slows down the process (Ding *et al.*, 2012; J. A. Gonzalez-Calderon *et al.*, 2016; Supaphol *et al.*, 2007).

Conclusions

From the results here presented, it is possible to conclude the following: the polarity and chemical nature of the side group of the alkoxy silane modifiers influence the crystallization process of the iPP. In addition, it was found that the amino group was the closest in similarity to the pure iPP.

In contrast, the other two groups, which had influential electronegative groups, presented recrystallization. This polarity affected their relative crystallinity, which was slower than the one of aminopropyl groups. The behavior here shown implied a greater Avrami exponent meaning a more gradual crystallization process. Finally, the activation energy was the lowest for the chloride group and the highest for glycidoxy, mainly due to the complex second crystallization process. All of what here is studied revealed that even if the siloxane coating was the same, the sole presence of high polarity groups attached to the layer is enough to stimulate a complex

crystallization of the aliphatic chains. Further studies are required to comprehend these interactions in non-aliphatic chains.

Acknowledgements

The authors express their gratitude to Consejo Nacional de Ciencia y Tecnología for the support of the Catedras-CONACYT program (J.A. Gonzalez-Calderon).

References

- Alariqi, S. A. S., Kumar, A. P., Rao, B. S. M., & Singh, R. P. (2009). Effect of γ -dose rate on crystallinity and morphological changes of γ -sterilized biomedical polypropylene. *Polymer Degradation and Stability* 94, 272-277. <https://doi.org/10.1016/j.polyimdegstab.2008.10.027>
- Allen, J. J., Rosenberg, E., Johnston, E., & Hart, C. (2012). Sol-Gel synthesis and characterization of silica polyamine composites: applications to metal ion capture. *ACS Applied Materials and Interfaces* 4, 1573-1584. <https://doi.org/10.1021/am201761m>
- Alyamac, E., Gu, H., Soucek, M. D., Qiu, S., & Buchheit, R. G. (2012). Alkoxysilane oligomer modified epoxide primers. *Progress in Organic Coatings* 74, 67-81. <https://doi.org/10.1016/j.porgcoat.2011.11.012>
- Auta, H. S., Emenike, C. U., & Fauziah, S. H. (2017). Distribution and importance of microplastics in the marine environment: A review of the sources, fate, effects, and potential solutions. *Environment International* 102, 165-176. <https://doi.org/10.1016/j.envint.2017.02.013>
- Blaine, R. L., & Kissinger, H. E. (2012a). Homer Kissinger and the Kissinger equation. *Thermochimica Acta* 540, 1-6. <https://doi.org/10.1016/j.tca.2012.04.008>
- Borovanska, I., Dobreva, T., Benavente, R., Djoumaliisky, S., & Kotzev, G. (2012). Quality assessment of recycled and modified LDPE/PP blends. *Journal of Elastomers and Plastics* 44, 479-497. <https://doi.org/10.1177/0095244312441731>
- Cao, J., Zuo, Y., Wang, D., Zhang, J., & Feng, S. (2017). Functional polysiloxanes: a novel synthesis method and hydrophilic applications. *New Journal of Chemistry* 41, 8546-8553. <https://doi.org/10.1039/C7NJ01294B>
- Chiellini, E., Corti, A., D'Antone, S., & Baciù, R. (2006). Oxo-biodegradable carbon backbone polymers - Oxidative degradation of polyethylene under accelerated test conditions. *Polymer Degradation and Stability* 91, 2739-2747. <https://doi.org/10.1016/j.polyimdegstab.2006.03.022>
- Chin, S., & Ai Tjong, S. (1997). Non-isothermal crystallization kinetics of calcium carbonate-filled b-crystalline phase polypropylene composites. *Polymer International* 46, 95-103. [https://doi.org/10.1002/\(SICI\)1097-0126\(199709\)46:1<95::AID-PI821>3.0.CO;2-L](https://doi.org/10.1002/(SICI)1097-0126(199709)46:1<95::AID-PI821>3.0.CO;2-L)
- Cho, S., Kim, N., Lee, S., Lee, H., Lee, S. H., Kim, J., & Choi, J. W. (2016). Use of hybrid composite particles prepared using alkoxysilane-functionalized amphiphilic polymer precursors for simultaneous removal of various pollutants from water. *Chemosphere* 156, 302-311. <https://doi.org/10.1016/j.chemosphere.2016.05.004>
- Chûjô, R., Kogure, Y., & Väänänen, T. (1994). Two-site model analysis of ^{13}C n.m.r. of polypropylene polymerized by Ziegler-Natta catalyst with external alkoxysilane donors. *Polymer* 35, 339-342.
- Connell, L. S., Gabrielli, L., Mahony, O., Russo, L., Cipolla, L., & Jones, J. R. (2017). Functionalizing natural polymers with alkoxysilane coupling agents: Reacting 3-glycidoxypropyl trimethoxysilane with poly(γ -glutamic acid) and gelatin. *Polymer Chemistry* 8, 1095-1103. <https://doi.org/10.1039/c6py01425a>
- Dai, X., Zhang, Z., Chen, C., Li, M., Tan, Y., & Mai, K. (2015). Non-isothermal crystallization kinetics of montmorillonite filled β -isotactic polypropylene nanocomposites. *Journal of Thermal Analysis and Calorimetry*

- 121, 829-838. <https://doi.org/10.1007/s10973-015-4635-8>
- Dai, X., Zhang, Z., Wang, C., Ding, Q., Jiang, J., & Mai, K. (2013). A novel montmorillonite with nucleating surface for enhancing-crystallization of isotactic polypropylene. *Composites Part A: Applied Science and Manufacturing* 49, 1-8. <https://doi.org/10.1016/j.compositesa.2013.01.016>
- Delgado Alvarado, E., Peña Juárez, M. G., Perez Perez, C., Perez, E., & Gonzalez, J. A. (2019). Improvement in the dispersion of TiO₂ particles inside Chitosan-Methyl cellulose films by the use of silane coupling agent. *Journal of the Mexican Chemical Society* 63. <https://doi.org/10.29356/jmcs.v63i2.741>
- Demir, H., Balköse, D., & Ülkü, S. (2006). Influence of surface modification of fillers and polymer on flammability and tensile behaviour of polypropylene-composites. *Polymer Degradation and Stability* 91, 1079-1085. <https://doi.org/10.1016/j.polymdegradstab.2005.07.012>
- Ding, Q., Zhang, Z., Wang, C., Jiang, J., Li, G., & Mai, K. (2012). Crystallization behavior and melting characteristics of wollastonite filled β -isotactic polypropylene composites. *Thermochimica Acta* 536, 47-54. <https://doi.org/10.1016/j.tca.2012.02.023>
- Dintcheva, N. T., Arrigo, R., Morici, E., Gambarotti, C., Carroccio, S., Cicogna, F., & Filippone, G. (2015). Multi-functional hindered amine light stabilizers-functionalized carbon nanotubes for advanced ultra-high molecular weight Polyethylene-based nanocomposites. *Composites Part B: Engineering* 82, 196-204. <https://doi.org/10.1016/j.compositesb.2015.07.017>
- Fuad, M. Y. A., Ismail, Z., Ishak, Z. A. M., & Omar, A. K. M. (1995). Application of rice husk ash as fillers in polypropylene: Effect of titanate, zirconate and silane coupling agents. *European Polymer Journal* 31, 885-893. [https://doi.org/10.1016/0014-3057\(95\)00041-0](https://doi.org/10.1016/0014-3057(95)00041-0)
- Gonzalez-Calderon, J. A., Vallejo-Montesinos, J., Almendarez-Camarillo, A., Montiel, R., & Pérez, E. (2016). Non-isothermal crystallization analysis of isotactic polypropylene filled with titanium dioxide particles modified by a dicarboxylic acid. *Thermochimica Acta* 631, 8-17. <https://doi.org/10.1016/j.tca.2016.03.007>
- Gonzalez-Calderon, J. A., Vallejo-Montesinos, J., Mata-Padilla, J. M., Pérez, E., & Almendarez-Camarillo, A. (2015). Effective method for the synthesis of pimelic acid/TiO₂ nanoparticles with a high capacity to nucleate β -crystals in isotactic polypropylene nanocomposites. *Journal of Materials Science* 50, 7998-8006. <https://doi.org/10.1007/s10853-015-9365-6>
- Gonzalez-Calderon, J. A., Vallejo-Montesinos, J., Almendarez-Camarillo, A., Montiel, R., & Pérez, E. (2016). Non-isothermal crystallization analysis of isotactic polypropylene filled with titanium dioxide particles modified by a dicarboxylic acid. *Thermochimica Acta* 631, 8-17. <https://doi.org/10.1016/j.tca.2016.03.007>
- Gonzalez-Calderon, J. A., Vallejo-Montesinos, J., Martínez-Martínez, H. N., Cerecero-Enríquez, R., & López-Zamora, L. (2019). Effect of chemical modification of titanium dioxide particles via silanization under properties of chitosan/potato-starch films. *Revista Mexicana de Ingeniería Química* 18, 913-927. Retrieved from www.rmiq.org
- Gonzalez-Calderon, José Amir, Pérez-Pérez, C., Pérez Rodríguez, R. Y., Fierro-González, J. C., & Vallejo-Montesinos, J. (2019). Silanization of di-n-octyldichlorosilane as a route to improve the integration of titanium dioxide in polypropylene. *Journal of Thermal Analysis and Calorimetry*. <https://doi.org/10.1007/s10973-019-08159-y>
- Gonzalez-Rodriguez, V., Escobar-Barrios, V., Peña-Juárez, M. G., & Pérez, E. (2020). Thermochimica Acta Effect of aliphatic chain in dicarboxylic acids on non-isothermal crystallization and mechanical behavior of titanium dioxide / iPP composites. *Thermochimica Acta* 686, 178543. <https://doi.org/10.1016/j.tca.2020.178543>
- González, A., Pérez, E., Almendarez, A., Villegas, A., & Vallejo-Montesinos, J. (2016). Calcium

- pimelate supported on TiO₂ nanoparticles as isotactic polypropylene prodegradant. *Polymer Bulletin* 73, 39-51. <https://doi.org/10.1007/s00289-015-1469-2>
- Habila, B., Ukoha, P. O., Okoduwa, S. I. R., Salim, A., Babangida, M. B., & Simon, A. (2020). Synthesis and characterization of an immobilized thiosalicylic-mercaptoethanol biligand system and its application in the detoxification of chromium(iii) and iron(iii) ions from tannery wastewater. *New Journal of Chemistry* 44, 2321-2327. <https://doi.org/10.1039/c9nj05072h>
- He, Z. L., Chen, L. N., Zhang, L., Ren, H. Y., Xu, M. Di, & Lou, Y. W. (2020). Effect of filler functional groups on the mechanical properties and relevant mechanisms of polydicyclopentadiene nanocomposites. *Journal of Applied Polymer Science*, 1-11. <https://doi.org/10.1002/app.49010>
- Huang, L., Wang, H., Wang, W., Wang, Q., & Song, Y. (2016). Non-isothermal crystallization kinetics of wood-flour/polypropylene composites in the presence of β -nucleating agent. *Journal of Forestry Research* 27, 949-958. <https://doi.org/10.1007/s11676-016-0209-2>
- Huang, M. -R, Li, X. -G, & Fang, B. -R. (1995). β -Nucleators and β -crystalline form of isotactic polypropylene. *Journal of Applied Polymer Science* 56, 1323-1337. <https://doi.org/10.1002/app.1995.070561014>
- Huber, M. P., Kelch, S., & Berke, H. (2016). FTIR investigations on hydrolysis and condensation reactions of alkoxy silane terminated polymers for use in adhesives and sealants. *International Journal of Adhesion and Adhesives* 64, 153-162. <https://doi.org/10.1016/j.ijadhadh.2015.10.014>
- Huo, H., Jiang, S., An, L., & Feng, J. (2004). Influence of Shear on Crystallization Behavior of the β Phase in Isotactic Polypropylene with β -Nucleating Agent. *Macromolecules* 37, 2478-2483. <https://doi.org/10.1021/ma0358531>
- Ijadpanah-saravi, H., Safari, M., & Khodadadi-darban, A. (2014). Synthesis of titanium dioxide nanoparticles for photocatalytic degradation of cyanide in wastewater. (November 2015). <https://doi.org/10.1080/00032719.2014.880170>
- Ismail, H., Mega, L., & Abdul Khalil, H. P. S. (2001). Effect of a silane coupling agent on the properties of white rice husk ash-polypropylene/natural rubber composites. *Polymer International* 50, 606-611. <https://doi.org/10.1002/pi.673>
- Issa, A. A., & Luyt, A. S. (2019). Kinetics of alkoxy silanes and organoalkoxy silanes polymerization: A review. *Polymers* 11. <https://doi.org/10.3390/polym11030537>
- Jagur-Grodzinski, J. (2006). Nanostructured polyolefins / clay composites: role of the molecular interaction at the interface. *Polym. Adv. Technol.* 17, 395-418. <https://doi.org/10.1002/pat>
- Ju, S.-P., Chen, C.-C., Huang, T.-J., Liao, C.-H., Chen, H.-L., Chuang, Y.-C., ... Chen, H.-T. (2016). Investigation of the structural and mechanical properties of polypropylene-based carbon fiber nanocomposites by experimental measurement and molecular dynamics simulation. *Computational Materials Science* 115, 1-10. <https://doi.org/10.1016/j.commatsci.2015.12.032>
- Karger-Kocsis, J. (1995). Polypropylene structure, blends and composites: Volume 3 *Composites*. Springer Netherlands.
- Kaya, D., McNally, T., Douglas, P., Coburn, N., & Gupta, J. (2018). Isothermal and non-isothermal crystallization kinetics of composites of poly(propylene) and MWCNTs. *Advanced Industrial and Engineering Polymer Research* 1, 99-110. <https://doi.org/10.1016/j.aiepr.2018.06.001>
- Kesmez, Ö. (2020). Hydrophobic, organic-inorganic hybrid sol-gel coatings containing boehmite nanoparticles for metal corrosion protection. *Chemical Papers* 74, 673-688. <https://doi.org/10.1007/s11696-019-00931-6>
- Kissinger, H. E. (1956). Variation of peak temperature with heating rate in differential thermal analysis. *Journal of Research of the National Bureau of Standards* 57, 217. <https://doi.org/10.6028/jres.057.026>

- Koch, K. M. (1983). Silane coupling agents. In *Journal of Organometallic Chemistry* (Vol. 246, pp. c27-c28). [https://doi.org/10.1016/S0022-328X\(00\)98664-9](https://doi.org/10.1016/S0022-328X(00)98664-9)
- Lee, C.-W., Joo, S.-W., & Gong, M.-S. (2005). Polymeric humidity sensor using polyelectrolytes derived from alkoxysilane cross-linker. *Sensors and Actuators B: Chemical* 105, 150-158. <https://doi.org/10.1016/j.snb.2004.05.037>
- Li, J. X., & Cheung, W. L. (1997). Pimelic acid-based nucleating agents for hexagonal crystalline polypropylene. *Journal of Vinyl and Additive Technology* 3, 151-156. <https://doi.org/10.1002/vnl.10182>
- Li, J. X., & Cheung, W. L. (1999). Conversion of growth and recrystallisation of β -phase in doped iPP. *Polymer* 40, 2085-2088. [https://doi.org/10.1016/S0032-3861\(98\)00425-X](https://doi.org/10.1016/S0032-3861(98)00425-X)
- Li, M., Li, G., Zhang, Z., Dai, X., & Mai, K. (2014). Enhanced β -crystallization in polypropylene random copolymer with a supported β -nucleating agent. *Thermochimica Acta* 598, 36-44. <https://doi.org/10.1016/j.tca.2014.11.004>
- López-Zamora, L., Martínez-Martínez, H. N., & González-Calderón, J. A. (2018). Improvement of the colloidal stability of titanium dioxide particles in water through silicon based coupling agent. *Materials Chemistry and Physics* 217, 285-290. <https://doi.org/10.1016/j.matchemphys.2018.06.063>
- Lotz, B. (1998). α and β phases of isotactic polypropylene: A case of growth kinetics "phase reentrancy" in polymer crystallization. *Polymer*, 39(19), 4561-4567. [https://doi.org/10.1016/S0032-3861\(97\)10147-1](https://doi.org/10.1016/S0032-3861(97)10147-1)
- Lv, Y., Huang, Y., Kong, M., & Li, G. (2013). Improved thermal oxidation stability of polypropylene films in the presence of β -nucleating agent. *Polymer Testing* 32, 179-186. <https://doi.org/10.1016/j.polymertesting.2012.10.008>
- Mani, M. R., Chellaswamy, R., Marathe, Y. N., & Pillai, V. K. (2016). New understanding on regulating the crystallization and morphology of the β -polymorph of isotactic polypropylene based on carboxylate-alumoxane nucleating agents. *Macromolecules* 49, 2197-2205. <https://doi.org/10.1021/acs.macromol.5b02466>
- Maryudi., Hisyam, A., Yunus, R., & Bag, M. (2013). Thermo-oxidative degradation of high density polyethylene containing manganese laurate. *International Journal of Engineering Research and Applications (IJERA)* 3, 1156-1165.
- Meer, S., Kausar, A., & Iqbal, T. (2016). Attributes of polymer and silica nanoparticle composites: a review. *Polymer-Plastics Technology and Engineering* 55, 826-861. <https://doi.org/10.1080/03602559.2015.1103267>
- Mendes, A. A., Cunha, A. M., & Bernardo, C. A. (2011). Study of the degradation mechanisms of polyethylene during reprocessing. *Polymer Degradation and Stability* 96, 1125-1133. <https://doi.org/10.1016/j.polymdegradstab.2011.02.015>
- Mendoza, G., Peña-Juárez, M. G., Perez, E., & Gonzalez-Calderon, J. A. (2020). Used of chemically modified titanium dioxide particles to mediate the non-isothermal cold crystallization of poly(lactic acid). *Journal of the Mexican Chemical Society* 64, 44-63. <https://doi.org/10.29356/jmcs.v64i2.1126>
- Muratov, D. S., Kuznetsov, D. V., Il'inykh, I. A., Burmistrov, I. N., & Mazov, I. N. (2015). Thermal conductivity of polypropylene composites filled with silane-modified hexagonal BN. *Composites Science and Technology* 111, 40-43. <https://doi.org/10.1016/j.compscitech.2015.03.003>
- Nocuń, M., Siwulski, S., Leja, E., & Jedliński, J. (2005). Structural studies of TEOS-tetraethoxytitanate based hybrids. *Optical Materials* 27, 1523-1528. <https://doi.org/10.1016/j.optmat.2005.01.014>
- Pantoja, M., Encinas, N., Abenojar, J., & Martínez, M. A. (2013). Effect of tetraethoxysilane coating on the improvement of plasma treated polypropylene adhesion. *Applied Surface Science* 280, 850-857. <https://doi.org/10.1016/j.apsusc.2013.05.074>
- Papageorgiou, G. Z., & Panayiotou, C. (2011). Crystallization and melting of biodegradable

- poly(propylene suberate). *Thermochimica Acta* 523, 187-190. <https://doi.org/10.1016/j.tca.2011.05.023>
- Raka, L., & Bogoeva-Gaceva, G. (2017). Crystallization of Polypropylene: Application of Differential Scanning Calorimetry Part I. Isothermal and Non-Isothermal Crystallization. *Contributions, Section of Natural, Mathematical and Biotechnical Sciences* 29, 69-87. <https://doi.org/10.20903/csnmbs.masa.2008.29.1-2.13>
- Reingruber, E., & Buchberger, W. (2010). Analysis of polyolefin stabilizers and their degradation products. *Journal of Separation Science* 33, 3463-3475. <https://doi.org/10.1002/jssc.201000493>
- Schneider, M. H., & Brebner, K. I. (1985). Wood-polymer combinations: The chemical modification of wood by alkoxysilane coupling agents. *Wood Science and Technology* 19, 67-73. <https://doi.org/10.1007/BF00354754>
- Shirosaki, Y., Tsuru, K., Hayakawa, S., Osaka, A., Lopes, M. A., Santos, J. D., ... Fernandes, M. H. (2009). Physical, chemical and *in vitro* biological profile of chitosan hybrid membrane as a function of organosiloxane concentration. *Acta Biomaterialia* 5, 346-355. <https://doi.org/10.1016/j.actbio.2008.07.022>
- Sterman, S., & Marsden, J. G. (1966). Silane coupling agents. *Industrial and Engineering Chemistry* 58, 33-37. <https://doi.org/10.1021/ie50675a010>
- Supaphol, P., Thanomkiat, P., Junkasem, J., & Dangtungee, R. (2007). Non-isothermal melt-crystallization and mechanical properties of titanium(IV) oxide nanoparticle-filled isotactic polypropylene. *Polymer Testing* 26, 20-37. <https://doi.org/10.1016/j.polymeresting.2006.07.011>
- Tang, J., Wang, Y., Liu, H., & Belfiore, L. A. (2004). Effects of organic nucleating agents and zinc oxide nanoparticles on isotactic polypropylene crystallization. *Polymer* 45, 2081-2091. <https://doi.org/10.1016/j.polymer.2003.11.046>
- Thamaphat, K., Limsuwan, P., & Ngotawornchai, B. (2008). Phase Characterization of TiO₂ Powder by XRD and TEM. *Kasetsart J. (Nat. Sci.)*, 42, 357-361.
- Thomas, S. P., Thomas, S., & Bandyopadhyay, S. (2009). Mechanical, atomic force microscopy and focussed ion beam studies of isotactic polystyrene/titanium dioxide composites. *Composites Part A: Applied Science and Manufacturing* 40, 36-44. <https://doi.org/10.1016/j.compositesa.2008.10.005>
- Tonda-Turo, C., Gentile, P., Saracino, S., Chiono, V., Nandagiri, V. K., Muzio, G., ... Ciardelli, G. (2011). Comparative analysis of gelatin scaffolds crosslinked by genipin and silane coupling agent. *International Journal of Biological Macromolecules* 49, 700-706. <https://doi.org/10.1016/j.ijbiomac.2011.07.002>
- Tong, T., Zhang, J., Tian, B., Chen, F., & He, D. (2008). Preparation and characterization of anatase TiO₂ microspheres with porous frameworks via controlled hydrolysis of titanium alkoxide followed by hydrothermal treatment. *Materials Letters* 62, 2970-2972. <https://doi.org/10.1016/j.matlet.2008.01.085>
- Uhlig, F., & Dortmund, D. (2000). Si NMR some practical aspects. *Inorganic Chemistry* 2, 208-222. <https://doi.org/10.1021/ja027509+>
- Vallejo-montesinos, J., Cesar, J., Martínez, L., Montejano-carrizales, J. M., Pérez, E., Pérez, J. B., & Almendárez, A. (2017). Passivation of titanium oxide in polyethylene matrices using polyelectrolytes as titanium dioxide surface coating. *Mechanics, Materials Science & Engineering* 8. <https://doi.org/10.2412/mmse.96.48.950>
- Vallejo-Montesinos, J., Muñoz, U. M., & Gonzalez-Calderon, J. A. (2016). Mechanical properties, crystallization and degradation of polypropylene due to nucleating agents, fillers and additives. In: *Polypropylene: Properties, Uses and Benefits*.
- Vallejo-Montesinos, Javier, Gámez-Cordero, J., Zarraga, R., Pérez Pérez, M. C., & Gonzalez-Calderon, J. A. (2019). Influence of the surface modification of titanium dioxide

- nanoparticles TiO₂ under efficiency of silver nanodots deposition and its effect under the properties of starch-chitosan (SC) films. *Polymer Bulletin*. <https://doi.org/10.1007/s00289-019-02740-z>
- Vyazovkin, S. (2002). Is the Kissinger equation applicable to the processes that occur on cooling? *Macromolecular Rapid Communications* 23, 771-775. [https://doi.org/10.1002/1521-3927\(20020901\)23:13<771::AID-MARC771>3.0.CO;2-G](https://doi.org/10.1002/1521-3927(20020901)23:13<771::AID-MARC771>3.0.CO;2-G)
- Wang, C., Zhang, Z., Du, Y., Zhang, J., & Mai, K. (2011). Effect of poly (styrene-co-acrylonitrile) on β -nucleation of polypropylene filled with supported β -nucleating agent. *Thermochimica Acta* 524, 157-164. <https://doi.org/10.1016/j.tca.2011.07.008>
- Wang, J., & Dou, Q. (2007). Non-isothermal crystallization kinetics and morphology of isotactic polypropylene (iPP) nucleated with rosin-based nucleating agents. *Journal of Macromolecular Science, Part B: Physics* 46, 987-1001. <https://doi.org/10.1080/00222340701457311>
- Wang, S., Ahmad, Z., & Mark, J. E. (1994). Polyimide-silica hybrid materials modified by incorporation of an organically substituted alkoxy silane. *Chemistry of Materials* 6, 943-946. <https://doi.org/10.1021/cm00043a013>
- Wright, S. L., Thompson, R. C., & Galloway, T. S. (2013). The physical impacts of microplastics on marine organisms: A review. *Environmental Pollution* 178, 483-492. <https://doi.org/10.1016/j.envpol.2013.02.031>
- Zhang, X., Do, M. D., & Bilyk, A. (2007). Chemical modification of wheat-protein-based natural polymers: Formation of polymer networks with alkoxy silanes to modify molecular motions and enhance the material performance. *Biomacromolecules* 8, 1881-1889. <https://doi.org/10.1021/bm070290c>
- Zhang, Z., Tao, Y., Yang, Z., & Mai, K. (2008). Preparation and characteristics of nano-CaCO₃ supported-nucleating agent of polypropylene. *European Polymer Journal* 44, 1955-1961. <https://doi.org/10.1016/j.eurpolymj.2008.04.022>
- Zhang, Z., Wang, C., Junping, Z., & Mai, K. (2012). β -Nucleation of pimelic acid supported on metal oxides in isotactic polypropylene. *Polymer International* 61, 818-824. <https://doi.org/10.1002/pi.4148>